

Transmission Matrix Representation of Finline Discontinuities

ABBAS SAYED OMAR AND KLAUS SCHÜNEMANN, MEMBER, IEEE

Abstract — A general treatise of cascaded discontinuities in inhomogeneous waveguides is given and applied to finline circuits. A transmission matrix representation is superior to a scattering matrix representation as far as CPU time is concerned. The scattering matrix is, however, advantageous if the sum of the line lengths separating the discontinuities is large. Numerical examples are given in order to illustrate the effect of increasing the number of modes used to represent the field at both sides of the discontinuity.

I. INTRODUCTION

THE PROBLEM OF electromagnetic scattering at waveguide discontinuities has been treated by many exact and approximate methods. The most general, rigorous, and systematic one is the modal expansion method, which has been used, e.g., in [1]–[4]. Its formulation for homogeneously filled waveguides differs from that for inhomogeneously filled waveguides. In the former case, the normal modes are either of the TE- or TM-type, so that the transverse magnetic-field vector of any mode is related to its transverse electric-field vector via the wave admittance. This simplifies the problem to some extent through the use of impedance and/or admittance matrices [3], [4]. In the latter case, the normal modes are of the hybrid type (i.e., linear combinations of TE and TM fields) so that wave impedances and/or admittances cannot be defined any longer. Both electric- and magnetic-field vectors should be used to characterize a hybrid mode. This general formulation has been presented, e.g., in [1], [2]. It will be followed here.

Microwave circuits usually consist of a large number of line sections that are separated by abrupt junctions. In the case of multisection finline bandpass filters, e.g., the dimensions of the slot pattern must be altered many times during the numerical design procedure until the required response curve is well approximated. Hence, saving CPU time is an important factor in system design. We will compare transmission and scattering matrix representations of cascaded junctions regarding this point. Another important factor in saving CPU time is the number of modes used to represent the field at both sides of the discontinuity. This factor will also be studied by comparison to measured data. Finline circuits are taken as a case

Manuscript received January 28, 1985; revised April 26, 1985. This work was supported in part by the Deutsche Forschungsgemeinschaft.

The authors are with the Technische Universität Hamburg-Harburg, Arbeitsbereich Hochfrequenztechnik, Postfach 90 14 03, D-2100 Hamburg 90, West Germany.

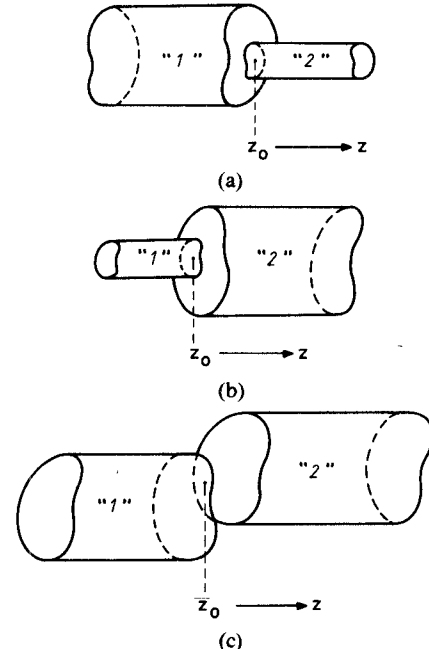


Fig. 1. Waveguide discontinuities of the (a) boundary-reduction-type, (b) boundary-enlargement-type, and (c) mixed-type.

study, although the results are general and can be applied to any other circuit technology.

II. BASIC FORMULATION

Most of the waveguide discontinuities have either of the forms shown in Fig. 1: a boundary-reduction-type [1], a boundary-enlargement-type [1], and a mixed-type discontinuity. Following [1] and [2], we will relate the complex amplitude vectors $\mathbf{a}^{(1)}$ and $\mathbf{a}^{(2)}$ of the incident modes to $\mathbf{b}^{(1)}$ and $\mathbf{b}^{(2)}$ of the scattered modes. Limiting the number of modes in guides "1" and "2" which are to be taken into account to N and M , respectively, both $\mathbf{a}^{(1)}$ and $\mathbf{b}^{(1)}$ can be written as N -dimensional column vectors and $\mathbf{a}^{(2)}$ and $\mathbf{b}^{(2)}$ as M -dimensional ones.

From the many orthogonality relations existing between the normal modes of uniform waveguides with perfectly conducting walls and lossless isotropic filling media, we use the following [5]:

$$\int_{(S_1)} (\mathbf{e}_n^{(1)} \times \mathbf{h}_m^{(1)*}) \cdot d\mathbf{s} = P_n \delta_{nm}$$

$$\int_{(S_2)} (\mathbf{e}_n^{(2)} \times \mathbf{h}_m^{(2)*}) \cdot d\mathbf{s} = Q_m \delta_{mn}. \quad (1)$$

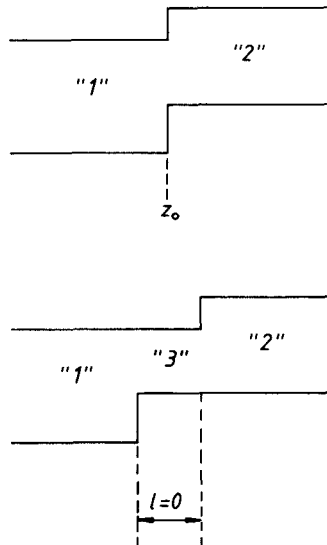


Fig. 2. Equivalence between a mixed-type discontinuity and two normal discontinuities in cascade.

Here, $\mathbf{e}_n^{(1)}$ and $\mathbf{h}_m^{(1)}$ are the transverse electric- and magnetic-field vectors of the n th and m th normal modes, respectively, in waveguide "1", $\mathbf{e}_n^{(2)}$ and $\mathbf{h}_m^{(2)}$ are the corresponding vectors in waveguide "2", δ_{nm} is the Kronecker delta, S_1 and S_2 are the cross sections of the corresponding guides, and "*" denotes "complex conjugate".

A. Boundary-Reduction and Boundary-Enlargement Discontinuities

The analysis of both types of discontinuities is essentially the same, so that we will give the equations describing the boundary-reduction-type (shown in Fig. 1(a)) only. By defining

$$A_{nm} = \int_{(S_2)} (\mathbf{e}_m^{(2)} \times \mathbf{h}_n^{(1)*}) \cdot d\mathbf{s},$$

$$n = 1, 2, \dots, N$$

$$m = 1, 2, \dots, M \quad (2)$$

the amplitude vectors of the incident and reflected modes can be related by the following two matrix equations:

$$[\lambda_P] \cdot (\mathbf{a}^{(1)} + \mathbf{b}^{(1)}) = [\mathbf{A}] \cdot (\mathbf{a}^{(2)} + \mathbf{b}^{(2)}) \quad (3a)$$

$$[\lambda_Q]^* \cdot (\mathbf{b}^{(2)} - \mathbf{a}^{(2)}) = [\mathbf{A}]^* \cdot (\mathbf{a}^{(1)} - \mathbf{b}^{(1)}) \quad (3b)$$

where

$[\lambda_P]$ is an $(N \times N)$ diagonal matrix with elements P_n ,

$[\lambda_Q]$ is an $(M \times M)$ diagonal matrix with elements Q_m ,

$[\mathbf{A}]$ is an $(N \times M)$ matrix with elements A_{nm} , and

$[\mathbf{A}]^{*t}$ means the conjugate transpose matrix of $[\mathbf{A}]$.

B. Mixed-Type Discontinuity

The type of discontinuity shown in Fig. 1(c) can be regarded as two cascaded junctions, the first between waveguides "1" and "3" being of the boundary-reduction-type, the second between waveguides "3" and "2" being of the boundary-enlargement-type. This equivalence has been sketched in Fig. 2. The length l of guide "3" is assumed to be zero.

This treatment is not in principle different from that proposed in [2], where the electromagnetic fields in waveguides "1" and "2" have independently been matched in the junction plane $z = z_0$ to a set of electric and magnetic vectors which is complete with respect to the common aperture between "1" and "2". In our formulation, this complete set is just the set of normal modes in waveguide "3" whose cross section equals the common aperture.

C. The Conservation of Complex Power

The continuity of complex power across a waveguide junction has been used in [3] to replace the matching condition for the transverse magnetic field. Furthermore, this principle has been shown in [4] to result from matching the transverse electric and magnetic fields in the junction plane. In both cases, the waveguides forming the junction were homogeneously filled. We will prove in the following that any of the relations originating from

- 1) matching the transverse electric field,
- 2) matching the transverse magnetic field,
- 3) the continuity of the complex power,

can be deduced from the other two.

This holds not only for junctions between homogeneously filled waveguides but also for the general case where the normal modes are of the hybrid-type.

For any of the junctions shown in Fig. 1, the continuity of the complex power is represented by the following relation:

$$(\mathbf{a}^{(1)} - \mathbf{b}^{(1)})^{*t} \cdot [\lambda_P] \cdot (\mathbf{a}^{(1)} + \mathbf{b}^{(1)}) =$$

$$(\mathbf{b}^{(2)} - \mathbf{a}^{(2)})^{*t} \cdot [\lambda_Q] \cdot (\mathbf{a}^{(2)} + \mathbf{b}^{(2)}). \quad (4)$$

As an example, the boundary-reduction case is considered, which is characterized by (3). These two equations represent, in fact, the matching of the electric and magnetic fields, respectively, at the junction, and can be used to verify (4). Inserting first (3a) and then (3b), we get

$$(\mathbf{a}^{(1)} - \mathbf{b}^{(1)})^{*t} \cdot [\lambda_P] \cdot (\mathbf{a}^{(1)} + \mathbf{b}^{(1)}) =$$

$$(\mathbf{a}^{(1)} - \mathbf{b}^{(1)})^{*t} \cdot [\mathbf{A}] \cdot (\mathbf{a}^{(2)} + \mathbf{b}^{(2)}) =$$

$$(\mathbf{b}^{(2)} - \mathbf{a}^{(2)})^{*t} \cdot [\lambda_Q] \cdot (\mathbf{a}^{(2)} + \mathbf{b}^{(2)}), \quad Q.E.D.$$

In a similar way, we can use any two equations of (3a), (3b), and (4) to deduce the third.

D. Scattering Matrix Representation

As an example, the boundary-reduction case will be treated. With

$$[\mathbf{R}] = [\lambda_P]^{-1} \cdot [\mathbf{A}]$$

$$[\mathbf{T}] = ([\lambda_Q]^{-1} \cdot [\mathbf{A}]^t)^*$$

$$(5)$$

(3) can be written as

$$\mathbf{a}^{(1)} + \mathbf{b}^{(1)} = [\mathbf{R}] \cdot (\mathbf{a}^{(2)} + \mathbf{b}^{(2)})$$

$$\mathbf{b}^{(2)} - \mathbf{a}^{(2)} = [\mathbf{T}] \cdot (\mathbf{a}^{(1)} - \mathbf{b}^{(1)}) \quad (6)$$

where $[R]$ represents an $(N \times M)$ matrix, $[T]$ an $(M \times N)$ matrix so that the first relation establishes N linear equations, the second M equations. Thus, $(N + M)$ variables can be expressed in terms of the other $(N + M)$ variables. In particular, it is impossible to express $\mathbf{a}^{(1)}, \mathbf{b}^{(1)}$ in terms of $\mathbf{a}^{(2)}, \mathbf{b}^{(2)}$ if $N \neq M$, because the former represent $(2N)$, the latter $(2M)$ variables. The most suitable choice of dependent and independent variables is to express $\mathbf{b}^{(1)}, \mathbf{b}^{(2)}$ in terms of $\mathbf{a}^{(1)}, \mathbf{a}^{(2)}$, each pair representing $(N + M)$ variables. This leads to the scattering matrix representation

$$\begin{bmatrix} \mathbf{b}^{(1)} \\ \mathbf{b}^{(2)} \end{bmatrix} = \begin{bmatrix} [S_{11}] & [S_{12}] \\ [S_{21}] & [S_{22}] \end{bmatrix} \cdot \begin{bmatrix} \mathbf{a}^{(1)} \\ \mathbf{a}^{(2)} \end{bmatrix} \quad (7)$$

with

$$\begin{aligned} [S_{11}] &= ([R][T] + [I])^{-1} \cdot ([R][T] - [I]), & \text{an } (N \times N) \text{ matrix} \\ [S_{12}] &= 2([R][T] + [I])^{-1} \cdot [R], & \text{an } (N \times M) \text{ matrix} \\ [S_{21}] &= [T]([I] - [S_{11}]), & \text{an } (M \times N) \text{ matrix} \\ [S_{22}] &= [I] - [T][S_{12}], & \text{an } (M \times M) \text{ matrix} \end{aligned} \quad (8)$$

and $[I]$ is the unity matrix.

At least one matrix inversion and five matrix multiplications have to be performed in order to compute the different submatrices of the scattering matrix.

E. Transmission Matrix Representation

The situation is much simpler for an equal number of modes in waveguides "1" and "2": $N = M$. Then one can relate the incident and reflected modes in each waveguide by the transmission matrix according to

$$\begin{bmatrix} \mathbf{a}^{(1)} \\ \mathbf{b}^{(1)} \end{bmatrix} = \begin{bmatrix} [U] & [V] \\ [V] & [U] \end{bmatrix} \cdot \begin{bmatrix} \mathbf{a}^{(2)} \\ \mathbf{b}^{(2)} \end{bmatrix} \quad (9)$$

with

$$\begin{aligned} [U] &= \frac{1}{2}([R] - [T]^{-1}) \\ [V] &= \frac{1}{2}([R] + [T]^{-1}). \end{aligned} \quad (10)$$

The computation of the submatrices $[U]$ and $[V]$ requires just one matrix inversion. Hence, it is faster than the computation of the submatrices of the scattering matrix. The only restriction is that an equal number of modes must be used at either side of the junction.

The network theory of multiple-port microwave networks developed in [6] uses both transmission and scattering matrices. Although the formulation with the transmission matrix seems to be quite general, it has been proven there that for the general case $M \neq N$ there exists a mathematical inconsistency. In what follows, we will give a deeper insight into the reasons.

Assume an $(N \times M)$ matrix $[A]$ is pre-multiplied by an $(M \times N)$ matrix $[B]$ in order to get a square matrix $[C]$ of order $(M \times M)$

$$[C] = [B] \cdot [A].$$

Then the M equations represented by the rows of $[C]$ are

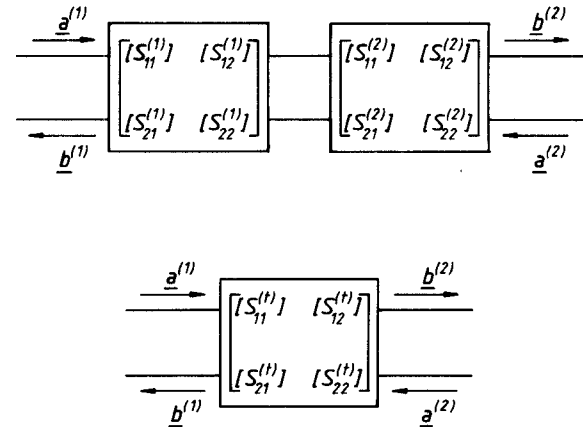


Fig. 3. Scattering matrix representation of cascaded discontinuities.

expressed as M linear combinations of the original N equations represented by the rows of $[A]$. Two cases must be distinguished.

1) $M < N$: Then one has lost all the information which is contained in the now missing $(N - M)$ equations, although $[C]$ may be inverted.

2) $M > N$: Then the additional $(M - N)$ equations are linearly dependent on the other N equations and $[C]$ is singular, i.e., it cannot be inverted.

In conclusion, it is important to know that matching N modes at one side of the discontinuity to M modes at the other always results in $(N + M)$ equations relating $2(M + N)$ variables. Hence, the only possibility is to express $(N + M)$ variables in terms of the other $(N + M)$ variables.

A further advantage of the transmission matrix representation is the easy handling of mixed-type discontinuities. The resulting submatrices $[U]$ and $[V]$ are then given by

$$\begin{aligned} [U] &= [V_\alpha][V_\beta] + [U_\alpha][V_\beta] \\ [V] &= [V_\alpha][V_\beta] + [U_\alpha][U_\beta]. \end{aligned} \quad (11)$$

Subscripts α and β refer to the junction between "1" and "3" and between "3" and "2", respectively.

F. Cascaded Discontinuities

In the case of cascaded discontinuities, there are two approaches. The first is to process the individual scattering matrices for calculating the overall scattering matrix. This approach has already been used for both the general case of interconnected multiports (e.g., in [7] and [8]) and the specific case of cascaded discontinuities (e.g., in [9]). Referring to Fig. 3, the submatrices forming the overall scattering matrix (superscript t) relating the reflected waves $\mathbf{b}^{(1)}, \mathbf{b}^{(2)}$ to the incident waves $\mathbf{a}^{(1)}, \mathbf{a}^{(2)}$ are given by

$$\begin{aligned} [S_{11}^{(t)}] &= [S_{11}^{(1)}] + [S_{12}^{(1)}][S_{11}^{(2)}][E][S_{21}^{(1)}] \\ [S_{12}^{(t)}] &= [S_{12}^{(1)}] \cdot ([I] + [S_{11}^{(2)}][E][S_{22}^{(1)}]) \cdot [S_{12}^{(2)}] \\ [S_{21}^{(t)}] &= [S_{21}^{(2)}][E][S_{21}^{(1)}] \\ [S_{22}^{(t)}] &= [S_{22}^{(2)}] + [S_{21}^{(2)}][E][S_{22}^{(1)}][S_{12}^{(2)}] \\ [E] &= ([I] - [S_{22}^{(1)}][S_{11}^{(2)}])^{-1}. \end{aligned} \quad (12)$$

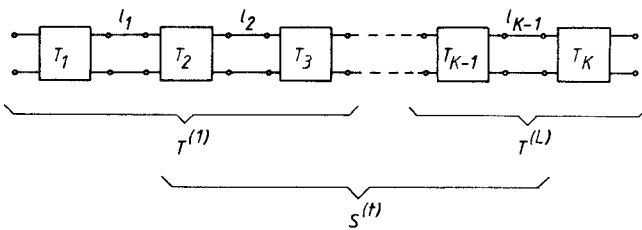


Fig. 4. Collecting discontinuities into groups which are cascaded by processing scattering matrices.

These calculations require at least one matrix inversion and ten matrix multiplications, if two discontinuities in cascade are to be treated.

The second approach can be applied only if equal numbers of modes are used for any of the guides. Then the individual transmission matrices can be processed. This requires eight matrix multiplications and no matrix inversion according to the following relations which can be derived from Fig. 3 (in which S should be thought to be replaced by T):

$$\begin{aligned} [T_{11}^{(1)}] &= [T_{11}^{(1)}][T_{21}^{(2)}] + [T_{12}^{(1)}][T_{11}^{(2)}] \\ [T_{12}^{(1)}] &= [T_{11}^{(1)}][T_{22}^{(2)}] + [T_{12}^{(1)}][T_{12}^{(2)}] \\ [T_{21}^{(1)}] &= [T_{21}^{(1)}][T_{21}^{(2)}] + [T_{22}^{(1)}][T_{11}^{(2)}] \\ [T_{22}^{(1)}] &= [T_{21}^{(1)}][T_{22}^{(2)}] + [T_{22}^{(1)}][T_{12}^{(2)}]. \end{aligned} \quad (13)$$

III. THE OVERFLOW PROBLEM

Cascaded discontinuities are always separated by uniform line sections, which may give rise to computational problems. Their scattering and transmission matrices are given by

$$\begin{aligned} [S] &= \begin{bmatrix} [0] & [\lambda_s] \\ [\lambda_s] & [0] \end{bmatrix} \\ [T] &= \begin{bmatrix} [0] & [\lambda_s]^{-1} \\ [\lambda_s] & [0] \end{bmatrix} \end{aligned} \quad (14)$$

with $[\lambda_s]$ a diagonal $(N \times N)$ matrix with elements

$$S_i = e^{-j\beta_i l}, \quad i = 1, 2, \dots, N$$

where β_i is the propagation constant of the i th mode of the uniform line and l is the line length.

Due to evanescent modes, $[\lambda_s]^{-1}$ usually contains very large numbers, which may lead to an overflow, in particular when multiplications have to be performed. These difficulties are only inherent to the transmission matrix representation if the sum of all separating line sections is much longer than the attenuation distance of the highest order mode which is taken into account. (The attenuation distance is defined as $1/|\beta_N|$.)

This situation can be circumvented if the cascaded discontinuities are collected into groups. Within each group the sum of the line sections must not be much longer than the attenuation distance. As has been sketched in Fig. 4, the cascaded discontinuities within each group are treated

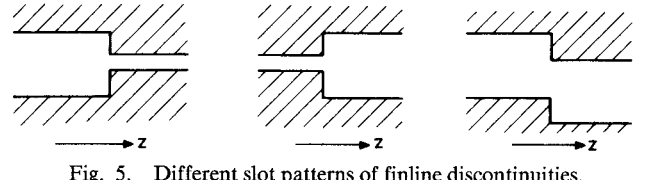


Fig. 5. Different slot patterns of finline discontinuities.

by applying the transmission matrix representation, while the groups are then cascaded within the scheme of scattering matrices. The number of groups L will always be much smaller than the number of junctions K , because long line lengths simultaneously reduce the number of higher order modes to be taken into account. The attenuation distance is then also long.

IV. APPLICATION TO FINLINES

For discontinuities between waveguides having the same housing as, e.g., finlines, shielded microstriplines, and suspended substrate lines, it has already been shown [9], [10] that there is no need to take different numbers of modes in the individual waveguide sections into account. Hence, the transmission matrix representation for cascaded discontinuities is by far the fastest one as far as computer time is concerned. Due to the finite thickness of the metal fins, three different junctions are imaginable (see Fig. 5): a decreasing (increasing) slot width corresponds to the boundary-reduction (enlargement) case, while a shift in the slot axis corresponds to the mixed-type problem. All these discontinuities should preferably be described by transmission matrices from the point of view of reducing the computation time. Saving CPU time is very important in optimizing finline slot patterns, e.g., in the case of band-pass filter or matching transformer design, where the slot width and section lengths are changed many times according to a suitable optimization algorithm until the system response approaches the specified one.

V. NUMERICAL RESULTS

The validity of our approach of analyzing mixed-type finline discontinuities has been checked by seeing whether the dominant mode scattering matrix is unitary. The fields on either side have been expanded into 5, 10, or 15 modes. The results in Table I show that this matrix is unitary irrespective of the number of modes. It should be noted that at the operating frequency, only the dominant modes on either side of the discontinuity are propagating.

The CPU time of both a transmission and a scattering matrix representation of cascaded discontinuities is shown in Table II. From this point of view, the former method is preferable in particular if the number of junctions increases.

The influence of the number of modes is finally illustrated by comparing the computed and the measured reflection coefficient of the finline structure shown in Fig. 6. Because this structure is lossless, the magnitude of the reflection coefficient Γ should be unity. This has been achieved computationally regardless of the number of modes used to expand the field at both sides of the discontinuity plane $z = 0$. The measured values have been

TABLE I
UNITARITY OF THE DOMINANT MODE SCATTERING MATRIX

Number of Modes	5	10	15
S_{11}	$+(0.401582) +j(0.048468)$	$+(0.419185) +j(0.025085)$	$+(0.414477) +j(0.068810)$
S_{12}	$+(0.912102) -j(0.066707)$	$+(0.900601) -j(0.112097)$	$+(0.900574) -j(0.111490)$
S_{21}	$+(0.912105) -j(0.066708)$	$+(0.900607) -j(0.112098)$	$+(0.900583) -j(0.111490)$
S_{22}	$-(0.390258) +j(0.106380)$	$-(0.400246) +j(0.127078)$	$-(0.385185) +j(0.167806)$
$S_{11} \cdot S_{11}^* + S_{12} \cdot S_{12}^*$	0.999997	0.999993	0.999990
$S_{21} \cdot S_{21}^* + S_{22} \cdot S_{22}^*$	1.000003	1.000005	1.000006
$S_{11} \cdot S_{21}^* + S_{12} \cdot S_{22}^*$	$+(0.000001) +j(0.000000)$	$+(0.000002) +j(0.000001)$	$+(0.000003) +j(0.000001)$

TABLE II
COMPARISON BETWEEN CPU TIME NEEDED FOR T - AND S -MATRIX FORMULATIONS

cpu-time in seconds		
number of junctions	T-matrix formulation	S-matrix formulation
1	30	46
2	65	106
3	109	171
4	150	246
5	183	310

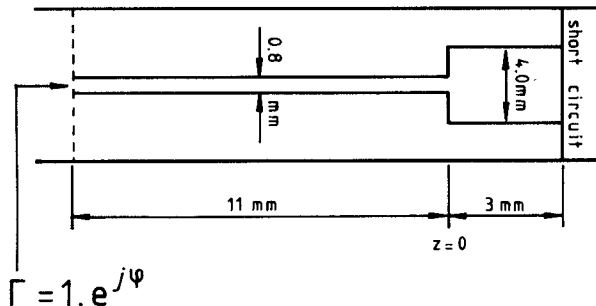


Fig. 6. The measured finline structure. Parameters: standard WR-62 housing, substrate thickness = 0.254 mm, $\epsilon_r = 2.22$.

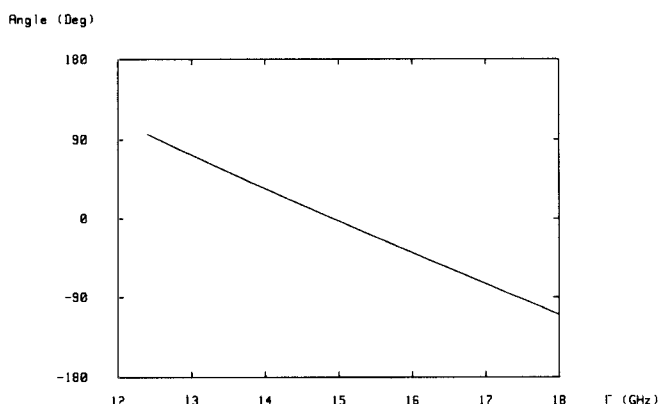


Fig. 7. Measured phase angle.

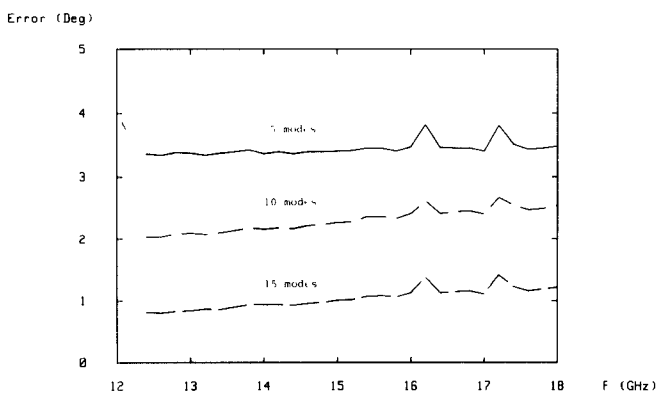


Fig. 8. Effect of the number of modes on the phase angle error.

obtained using an automatic network analyzer PASCAL program with 8-term correction implemented on an HP 9816 computer in conjunction with an HP 8410 C network analyzer. The magnitude of the measured reflection coefficient did not exceed -0.1 dB over the Ku-band (12.4–18 GHz). The phase of the measured reflection coefficient is shown in Fig. 7, the phase error in Fig. 8. It can be concluded then that a number of modes between 10 and 15 is quite sufficient for the field expansion.

ACKNOWLEDGMENT

The authors thank C. Bühst for preparing the manuscript.

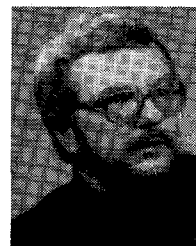
REFERENCES

- [1] A. Wexler, "Solution of waveguide discontinuities by modal analysis," *IEEE Trans. Microwave Theory Tech.*, vol. MTT-15, pp. 508–517, Sept. 1967.
- [2] P. H. Masterman and P. J. B. Clarricoats, "Computer field-matching solution of waveguide transverse discontinuities," *Proc. Inst. Elec. Eng.*, vol. 118, no. 1, pp. 51–63, Jan. 1971.
- [3] R. Safavi-Naini and R. H. Macphie, "On solving waveguide junction scattering problems by the conservation of complex power technique," *IEEE Trans. Microwave Theory Tech.*, vol. MTT-29, pp. 337–343, Apr. 1981.
- [4] H. Auda and R. F. Harrington, "A moment solution for waveguide junction problems," *IEEE Trans. Microwave Theory Tech.*, vol. MTT-31, pp. 515–520, July 1983.
- [5] R. E. Collin, *Field Theory of Guided Waves*. New York: McGraw-Hill, 1960.
- [6] H. Brand, "Schaltungslehre linearer Mikrowellennetze," *S. Hirzel Verlag*, 1970.
- [7] G. Filipsson, "A new general computer algorithm for S-matrix calculation of interconnected multiports," in *Proc. 11th EuMC* (Amsterdam), 1981, pp. 700–704.
- [8] G. R. Simpson, "A generalized n-port cascade connection," in *Proc. IEEE MTT-S Symp.* (Los Angeles), 1981, pp. 507–509.
- [9] L. P. Schmidt, "Zur feldtheoretischen Berechnung von transversalen Diskontinuitäten in Mikrostrip-Leitungen," Dr.-Ing. dissertation, Rheinisch-Westfälische Technische Hochschule Aachen, Aachen, West Germany, July 1979.
- [10] R. Mittra and S. W. Lee, *Analytical Techniques in the Theory of Guided Waves*. New York: Macmillan, 1971.



Abbas Sayed Omar was born in Sharkieh, Egypt, on December 9, 1954. He received the B.Sc. and M.Sc. degrees in electrical engineering from Ain Shams University, Cairo, Egypt, in 1978 and 1982, respectively.

From 1978 to 1982, he served as a Research and Teaching Assistant at the Department of Electronics and Computer Engineering of Ain Shams University, where he was engaged in investigations of microstriplines and below-cutoff waveguides and their use as a hybrid circuit technique for the realization of broad-band tunable oscillators. From 1982 to 1983, he joined the Institut für Hochfrequenztechnik, Technische Universität Braunschweig, Braunschweig, West Germany, as a Research Engineer, where he was involved with theoretical investigations on finlines. Since then he has held the same position at the Technische Universität Hamburg-Harburg, Hamburg, West Germany, where he is working towards the Doktor-Ing. degree. His current fields of research are the theoretical investigations of planar structures and dielectric resonators.



Klaus F. Schünemann (M'76) was born in Braunschweig, Germany, in 1939. He received the Dipl.-Ing. degree in electrical engineering and the Doktor-Ing. degree from Technische Universität Braunschweig, Germany, in 1965 and 1970, respectively.

Since 1983, he has been a Professor of Electrical Engineering and Director of the Arbeitsbereich Hochfrequenztechnik at the Technische Universität Hamburg-Harburg, Germany.

He has worked on nonlinear microwave circuits, diode modeling, solid-state oscillators, PCM communication systems, and integrated-circuit technologies such as finline and waveguides below cutoff. His current research interests are concerned with transport phenomena in submicron devices, CAD of planar millimeter-wave circuits, opto-electronics, and gyrotrons.